

HIRES Spectroscopy of Magnetic White Dwarfs

by

Mark M^cAnerin

A THESIS SUBMITTED IN PARTIAL FULFILMENT OF
THE REQUIREMENTS FOR THE DEGREE OF

Bachelor of Science

in

The Faculty of Science

(Physics and Astronomy)

The University Of British Columbia

June, 2007

© Mark M^cAnerin 2007

Abstract

The atmospheres of magnetic white dwarfs behave as theoretical analogues to neutron stars. The magnetic fields strengths and effective temperatures of the white dwarfs with the strongest magnetic fields are both two to three orders of magnitude below neutron stars. So the expectation is that their atmospheres and stellar envelopes will be as difficult to model as neutron stars due to the high degree of anisotropy in the thermal conduction through their atmospheres and envelopes. The construction of spectra and analyzing their absorption features with data taken with the HIRES instrument on Keck-I, could better constrain the models for all magnetic stellar atmospheres. Using the response transfer method of reducing echelle spectra we have created complete relative flux spectra of several magnetic white dwarf targets. Our reference in the reduction is Van Maanen 2, which behaves as a good blackbody and is devoid of spectral features above 4000\AA . Errors between orders due to the limitations of our method have prevented assembly of complete continuous spectra, but spectral data seems to indicate that there ranges of spectra up to several hundred angstroms wide with low systematic error, allowing analysis of the large spectral features of magnetic white dwarfs.

Table of Contents

| | |
|---|-----|
| Abstract | ii |
| Table of Contents | iii |
| List of Tables | iv |
| List of Figures | v |
| Acknowledgements | vi |
| 1 Introduction | 1 |
| 1.1 Magnetic White Dwarfs | 1 |
| 1.2 HIRES | 2 |
| 2 Data Reduction Methods | 5 |
| 2.1 Reference Spectra | 5 |
| 2.2 Theoretical Modelling | 5 |
| 2.3 Response Transfer | 6 |
| 3 Calculation and Results | 8 |
| 4 Discussion and Conclusions | 17 |
| Bibliography | 18 |

List of Tables

| | | |
|-----|--|----|
| 1.1 | Magnetic White Dwarf Targets | 2 |
| 3.1 | Day 1 Smoothed Conversion Ratio Coefficients | 10 |

List of Figures

| | | |
|-----|--|----|
| 1.1 | Light Path through the HIRES instrument | 3 |
| 1.2 | Example CCD image of a cross dispersed echelle spectrum . . | 3 |
| 3.1 | The 10th spectral order of Van Maanen 2 before reduction . . | 11 |
| 3.2 | The 10th spectral order of the reference spectra | 12 |
| 3.3 | The 10th spectral order of the unsmoothed conversion ratio . | 13 |
| 3.4 | The 10th spectral order of the conversion ratio | 14 |
| 3.5 | The 10th spectral order of Van Maanen 2 after data reduction | 15 |
| 3.6 | Spectral orders 20, 21, 22 of PG1015+014 | 16 |

Acknowledgements

Many thanks go to Dr. Jeremy Heyl, my supervisor, for always pointing me in the right direction whenever I lost my way with this project. Whether it was help with the daily struggles with IDL and other pieces of software or a good reference book, he was always seemed to have an answer.

I'd also like to thank the Theoretical High-Energy Astrophysics group at UBC for the use of their Tabitha and even putting me on the webpage as a member.

Myself, and I'm sure Dr. Heyl, wish to recognize and acknowledge the very significant cultural role and reverence that the summit of Mauna Kea has always had within the indigenous Hawaiian community. We are most fortunate to have been able to conduct observations from the mountain.

Chapter 1

Introduction

1.1 Magnetic White Dwarfs

Since the late 30's, magnetic white dwarfs have been studied due to their unusual absorption features. The positions of the hydrogen absorption lines in the spectra are perturbed from their normal positions to positions dictated by the stationary points of the wavelength of hydrogen atom transitions, which are dependant on magnetic field strength. [1]

The white dwarfs that we studied are highly magnetized. Their magnetic fields are measured by the position in their spectrum of absorption features, which are often significantly altered from their unperturbed positions. White dwarf magnetic fields above 10^5 are found to be evenly distributed in strength up to 10^9 G, far stronger than most white dwarfs. [7][6] These white dwarfs with strong magnetic fields can be thought of as analogues to neutron stars, in that their effective (surface) temperatures and magnetic field strength are both two orders of magnitude less than neutron stars. This means the ratio of these two values is approximately the same for these two classes of compact objects. [3]

The magnetic field-temperature ratio represents the degree of anisotropy in electron phase space. In natural units for magnetic field and temperature, $\beta/\tau \approx 134B/T$ (B and T in units of MG and K). For neutron stars, this is $B \approx 10^{11-12}$ G and $T \approx 10^{6-7}$ K. So the ratio for neutron stars $\beta/\tau \approx 10$. [3]

With the ratio being approximately the same between neutron stars and strongly magnetic white dwarfs, we expect the thermal conduction through magnetic white dwarf atmospheres to be as complicated and challenging to model as neutron stars. So studying magnetic white dwarfs can give us insight in the modelling of neutron star atmospheres and envelopes. Our magnetic dwarf targets and some of their properties are given in Table 1.1.

Some of our target stars also have noted periodicities in their luminosity, as noted in the Table 1.1. These may be linked to changes in their magnetic field strength as well which if true would correspond to shifts in absorption features in their spectra. Several exposures were taken of these targets and high resolution spectra would allow the construction of precise time-resolved

| Name | Period | T_{eff} (K) | B (MG) | β/τ |
|---------------|------------------|----------------------|----------|--------------|
| PG 1031+234 | 3.4 ^h | 15000 | 1000 | 8.96 |
| SBS 1349+5434 | — | 11000 | 760 | 9.28 |
| LB 11146 | — | 15000 | 670 | 6.00 |
| LP 790-29 | — | 8600 | 200 | 3.12 |
| PG 1015+014 | 1.7 ^h | 14000 | 120 | 1.15 |
| G 195-19 | 1.3 ^d | 8000 | 100 | 1.68 |

Table 1.1: Magnetic White Dwarf Targets [7] [3]

spectra of these targets.

1.2 HIRES

Our observations were taken on HIRES, the high resolution echelle spectrometer, a cross-dispersed echelle spectrograph mounted on the nasmyth platform of the Keck-I telescope at Mauna Kea, Hawaii. This instrument is designed to use the Keck telescope's ten-meter diameter to take very high signal-to-noise ratio measurements across a wide range of wavelengths including the entire visual spectrum and portions of the near-infrared and ultraviolet. [10] [9] [5]

The instrument provides such high resolution by using an echelle grating, a diffraction grating with a steep step-profile. The grating produces a series of overlapping high resolution spectral orders about 60Å long. A second, low-dispersion grating, called a cross disperser, with grooves perpendicular to the echelle grating is used to separate the overlapping spectral orders out onto a single CCD. A cartoon of the lightpath is given in Fig. 1.1 An example of a cross dispersed echelle CCD image is Fig. 1.2. [5]

These CCD images are preprocessed (debiased, flatfielded, and wavelength calibrated) into a more accessible format by a piece of software developed by the Keck observatory called MAKEE. This program reduces the CCD image into relative flux and wavelength information across each spectral order. The data is binned into $\approx 0.03\text{\AA}$ pieces, giving 2046 data points, per spectral order. Our data set contains information from 28 spectral orders, and a total range of about 2000Å. [10]

The trade-off for is the large non-linear response of the instrument on several scales. Both within each spectral order as well as across each gap of orders there are up to 10% errors which must be removed by calibration.

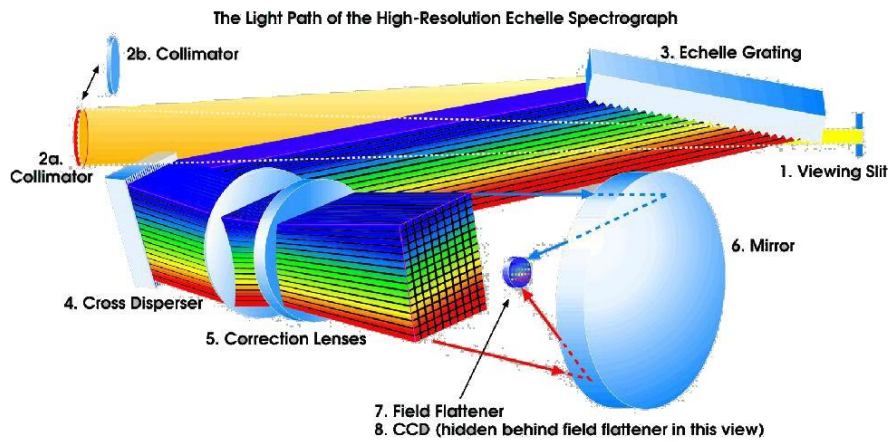


Figure 1.1: The light path through the HIRES instrument. [5]



Figure 1.2: An example CCD image of cross dispersed echelle spectrum separated out into spectral orders with the range of wavelengths displayed. [5]

Fortunately there is a small overlap of wavelengths at the beginning and end of each order, which are used to match orders together by setting these overlaps equal and shifting the neighbouring orders to match them up. [8]

Chapter 2

Data Reduction Methods

2.1 Reference Spectra

The normal method for reducing HIRES echelle spectra was developed by Suzuki et al [8]. It uses a well calibrated reference spectrum combined with the HIRES data to develop a continuous spectra with the overall shape of the reference spectra while including the high resolution detail of HIRES information.

The method relies on reducing the HIRES data's resolution to match the reference spectra, and rebinning the data to compare them. A low resolution conversion ratio between the reference and HIRES spectra can be created to both relate the reference spectra fluxes and the HIRES fluxes as well as force the HIRES data to follow the overall shape of the light curve of the reference. This conversion ratio is then fitted with a polynomial fit to remove low resolution spectral features that may remain from reference. Depending on the amount of structure in the spectrum, different types of polynomials or different degrees polynomial may be appropriate for different spectral orders. [8]

That conversion ratio is then binned back to HIRES resolution using the polynomial coefficients and divided from the full HIRES spectra. This results in the HIRES spectra matching the light curve of the reference, but with the absorption features of the HIRES data.

This method is highly successful but dependant on a well-calibrated reference spectra to match the HIRES data for every target. Unfortunately, we lack reference spectra to apply this method to any of our target stars so alternatives must be explored.

2.2 Theoretical Modelling

Another method of analyzing echelle data is to compare the data to a known stellar model. This method can be successful over short wavelength ranges if the features being studied are small compared to the size of a spectral

order and the features exhibit large flux differences from the surrounding high area. This method may be appropriate for analyzing such things as the widths and profiles of prominent spectral lines.

For a small area of interest, possibly as large as a few angstroms, the non-linearity in that area can be considered a small perturbation. This allows a theoretical model to be used as a reference level for the feature with the studied spectral feature being much larger than local non-linearities in the response. Something as simple as a fitted low order curve could be used as a baseline for an spectral feature due to the extremely short range of wavelengths under consideration. [9]

This method is feasible only over very short wavelength spans and with a specific feature that you wish to be studied. While our targets spectra were observed over a range of 2000Å, there are absorption features which span tens of angstroms making this method inappropriate for our use.

2.3 Response Transfer

Due to a lack of reference spectra, we elected to use a combination of these two methods to achieve the goal of spectral construction. A non-magnetic white dwarf, Van Maanen 2 (vMA2), was observed both nights that our data was taken. Van Maanen 2 is notable for it's lack of spectral features above 4000Å, especially its lack of hydrogen or helium lines. This makes this white dwarf an excellent blackbody in this spectral range. [2] [11]

Since Van Maanen 2's light curve behaves approximately as a blackbody, we can generate a set of reference fluxes using Planck's Law (Eq. 2.1) above 4000Å. Below 4000Å there are multiple absorption features in the spectra, including two very strong carbon absorption lines in the near ultraviolet, because they are not included in our reference we must trim out the range below 4000Å. Unfortunately this is almost 25% of our data. [11]

$$I(\lambda, T) = \frac{2hc^2}{\lambda^5} \frac{1}{\exp \frac{hc}{\lambda kT} - 1} \quad (2.1)$$

Using extracted wavelength information for vMA2 and knowing it's effective temperature to be 6750 K, we apply Planck's Law and built an appropriately binned reference spectrum. Only the relative overall shape of the curve is necessary due to our interest being a relative flux calibration, a spectrum that is only an overall normalization factor away from being a calibrated absolute flux spectra. Our theoretical reference light curve is then

used to build a conversion ratio using the reference spectra method outlined above. [2]

Smoothing across each spectral order with a low order polynomial fit and trimming the data below 4000Å removes any artifacts in the vMA2 data from short scale non-linearity in response. This conversion ratio is then applied to our magnetic white dwarf targets spectra taken the same evening to get a relative flux calibrated reference.

The validity of using a conversion ratio from a different star for our science targets is questionable. The reason echelle spectra are so difficult to calibrate is that the non-linearities can change on time scales that may be short compared to an evening's observations, especially when observing multiple targets. This method is well known for magnifying relative flux errors by compounding the small flux errors multiple times into the final results. [8]

Joining spectral orders into a continuous spectra from this method is also suspect. This method also tends to bias the removal of instrumental response in the middle of each spectral order over the edges. Unfortunately the largest non-linear areas are the near the edges of each spectral order, and the jumps between them. This method can leave 5-10% errors towards the edges of each spectral order and as much as 10% errors for the jumps between spectral orders, where discontinuities may occur in the worst cases. Thankfully the the relative flux is calibrated well in the middle of each order, so studying some spectral properties is still possible. [8]

Chapter 3

Calculation and Results

We used the above described response transfer method to our reduce our data. We have constructed, order by order, complete yet uncombined spectra of our target white dwarfs. Across individual orders, we were successful in removing the non-linear nature of the echelle spectrometer. Unfortunately, due to the polynomial fit's equal weighting (as we have no error information other than photon noise which is equal point to point), the polynomial fit has preferentially removed instrumental response at the center of spectral orders. This has caused large errors to develop at the edges of some spectral orders depending on the amount of structure contained within each order.

Although we were able to match the relative flux order to order, the spectra is not smooth as it should be. There are clear errors order to order as the polynomial fits naturally diverge from the conversion ratio at either end of the spectral order. The polynomial fits of neighbouring orders often diverge in opposite directions, this causes the first derivative of the light curve with respect to wavelength to be different order to order in the small regions of overlapping wavelength. Even the polynomial coefficients order to order change enough to be same magnitude but with the opposite sign in some cases. While a full spectrum could not be constructed, there are regions where the spectral orders can be joined in a well behaved manner.

An outline of the involved calculation follows, with illustrative figures of the various intermediate steps following:

1. The raw data is extracted within from a standard echelle .FITS (CCD image) file, flux information is pulled from the image itself while the wavelength information is stored in the header of the fits file and extracted seperately. (Fig. 3.1)
2. From the wavelength information, we construct the reference spectra using Planck's Law (Eqn. 2.1). This creates a reference flux, for every data point. (Fig. 3.2)
3. Individually dividing each reference data point by the raw fluxes at

their associated wavelengths produces the unsmoothed conversion ratio.(Fig. 3.3)

4. Fitting a polynomial to the unsmoothed conversion factor for each spectral order creates the smooth conversion factor for that spectral order. We decided on a 3rd order polynomial because it appears to be a working middle ground between the large scale and small scale response of the instrument. The polynomial fit results in an array of 112 coefficients, 4 per spectral order. The first night of observations polynomial coefficients are given in Table. 3.1. These coefficients are then evaluated in simple polynomial form (Eqn. 3.1) to create the final smoothed conversion ratio. (Fig. 3.4)
5. Multiplying the raw data by the conversion ratio ideally removes all instrument response and produces a relative flux spectral order which can then be joined to its neighbours to create a continuous relative flux spectra. If necessary the spectra can then be renormalized to an absolute flux spectra simply by a multiplicative factor. (Fig. 3.5)

$$CR(\lambda) = C[0] + C[1]\lambda + C[2]\lambda^2 + C[3]\lambda^3 \quad (3.1)$$

Due to the sheer amount of data involved in the results of even a single HIRES integration it is impractical to display a full spectrum in any form other than digital. Below are three orders joined together from PG1015+014 (Fig. 3.6), one of our magnetic white dwarf targets. Centered on order 21 an absorption line displaying the characteristic spreading that occurs in strong magnetic fields is apparant.

| Spectral Order | C[0] | C[1] | C[2] | C[3] |
|----------------|--------------|--------------|----------|----------|
| 0 | 7899.73 | -13.3958 | 0.00688 | 0.0 |
| 1 | -5.23320e+08 | 425719. | -115.430 | 0.01043 |
| 2 | -8.76186e+09 | 6.91739e+06 | -1820.38 | 0.15968 |
| 3 | -1.74316e+09 | 1.35794e+06 | -352.593 | 0.03052 |
| 4 | 5.44198e+10 | -4.21197e+07 | 10866.3 | -0.93443 |
| 5 | 1.52410e+11 | -1.16648e+08 | 29759.1 | -2.53068 |
| 6 | 1.36550e+10 | -1.03290e+07 | 2604.39 | -0.21890 |
| 7 | 1.29829e+09 | -979660. | 246.420 | -0.02066 |
| 8 | 1.69294e+09 | -1.25814e+06 | 311.679 | -0.02574 |
| 9 | 5.65796e+08 | -418109. | 102.994 | -0.00846 |
| 10 | 3.39148e+08 | -248023. | 60.4630 | -0.00491 |
| 11 | -9.96050e+08 | 709953. | -168.665 | 0.01336 |
| 12 | -2.75957e+08 | 193144. | -45.0496 | 0.00350 |
| 13 | -2.91256e+08 | 201940. | -46.6648 | 0.00359 |
| 14 | -9.63505e+08 | 662994. | -152.065 | 0.01163 |
| 15 | -7.87600e+08 | 534907. | -121.092 | 0.00914 |
| 16 | -8.37957e+08 | 561800. | -125.546 | 0.00935 |
| 17 | -9.94092e+08 | 658668. | -145.467 | 0.01071 |
| 18 | -7.94577e+08 | 519164. | -113.062 | 0.00821 |
| 19 | -8.56270e+08 | 552633. | -118.878 | 0.00852 |
| 20 | -3.53654e+08 | 224345. | -47.4282 | 0.00334 |
| 21 | 8.68006e+07 | -57232.5 | 12.5619 | -0.00092 |
| 22 | 5.12323e+08 | -321613. | 67.2995 | -0.00469 |
| 23 | 3.06929e+08 | -190939. | 39.5954 | -0.00274 |
| 24 | 4.87957e+08 | -296510. | 60.0649 | -0.00406 |
| 25 | 2.69026e+08 | -161758. | 32.4253 | -0.00217 |
| 26 | 2.42011e+08 | -143325. | 28.2988 | -0.00186 |
| 27 | 1.16727e+08 | -67807.1 | 13.1335 | -0.00085 |

Table 3.1: Day 1 Conversion Ratio Coefficients

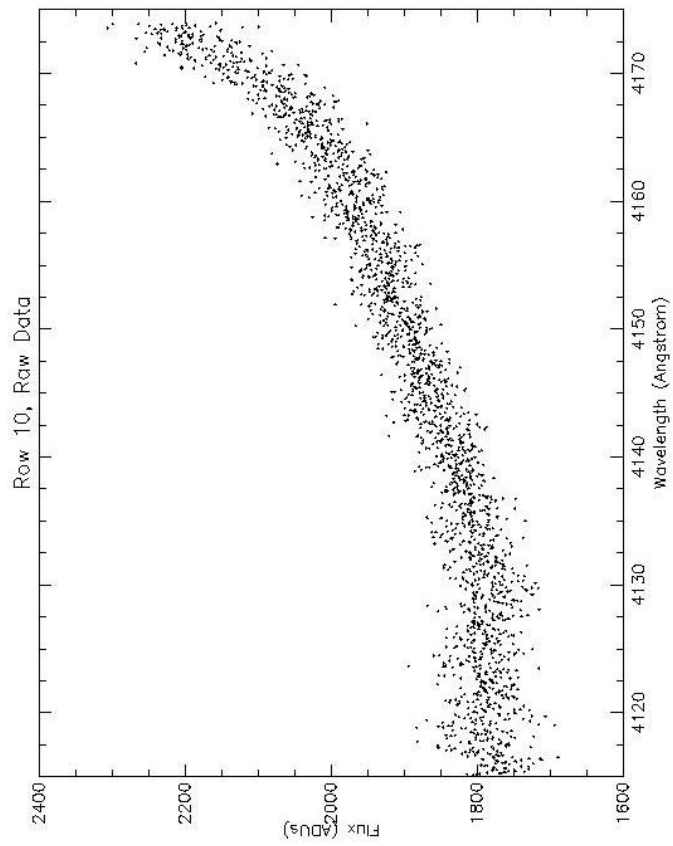


Figure 3.1: The 10th spectral order of Van Maanen 2, before any data reduction.

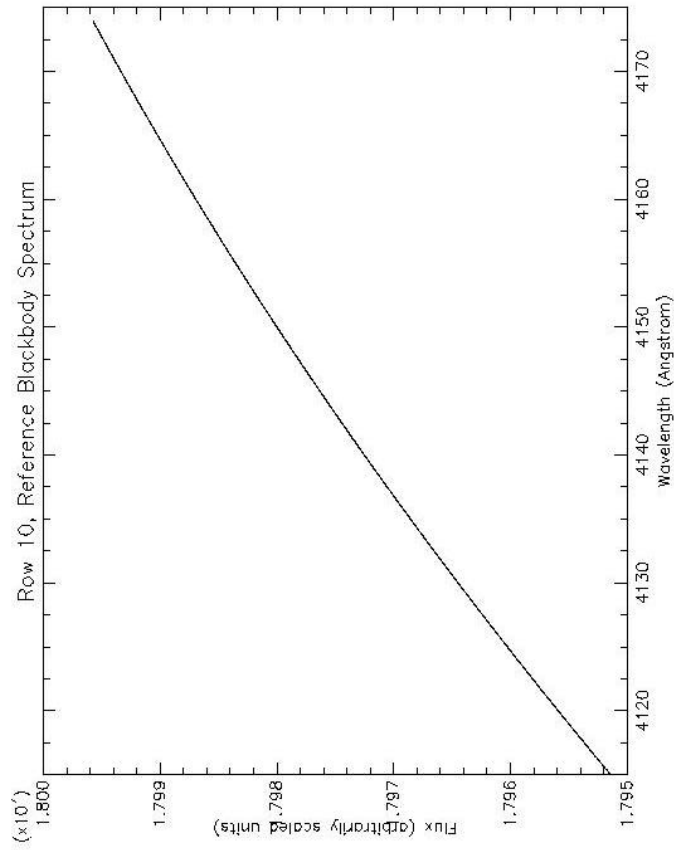


Figure 3.2: The 10th spectral order the theoretical reference spectra, built off of the wavelengths of the 10th spectra order of vMA2 using Planck's Law.

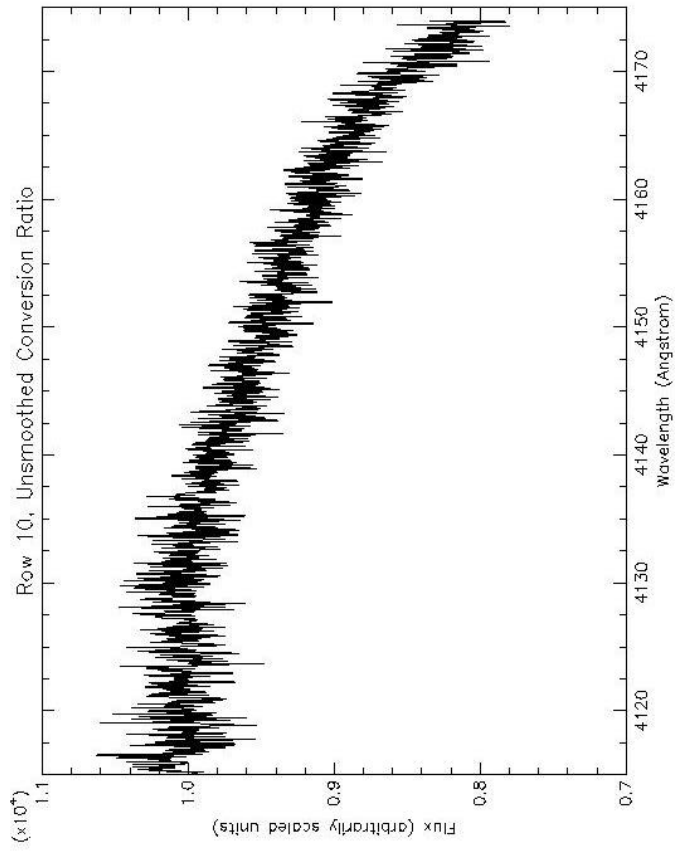


Figure 3.3: The 10th spectral order of the unsmoothed conversion ratio.

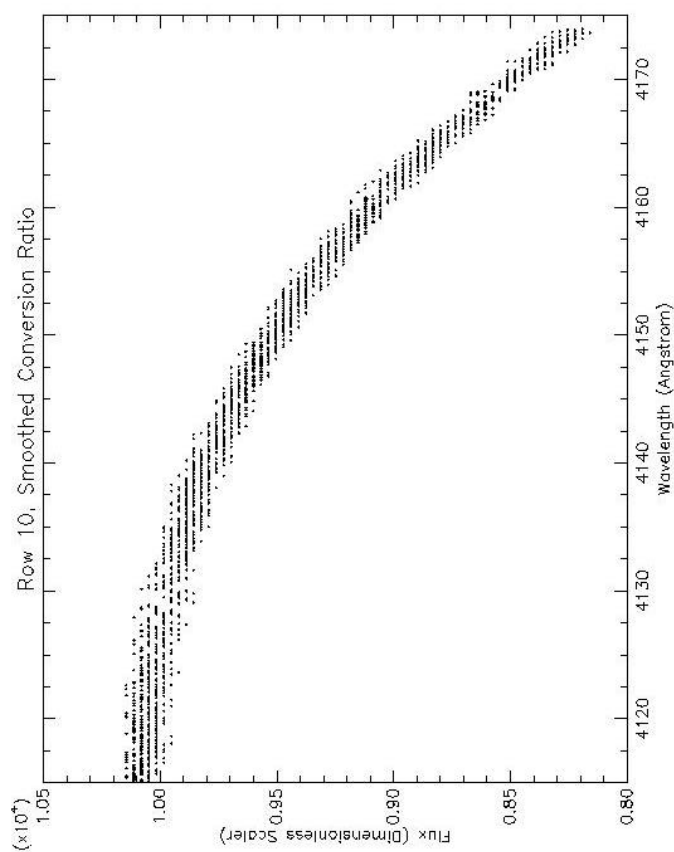


Figure 3.4: The 10th spectral order of the conversion ratio after being smoothed by the application of a 3rd order polynomial. The pattern in the image is the periodicity of the wavelength bins, which are not all exactly equal in size but very on the order of 0.01\AA .

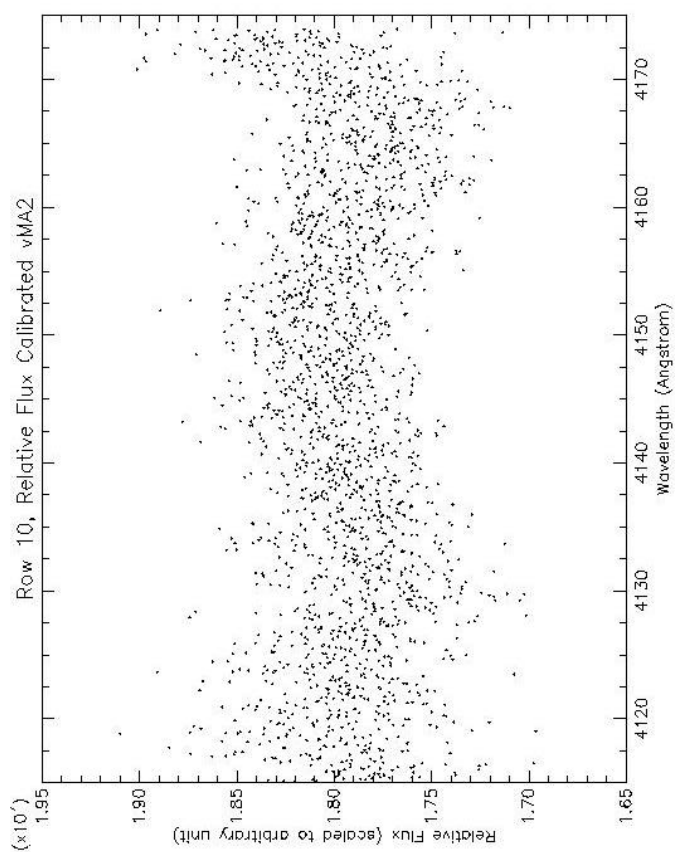


Figure 3.5: The 10th spectral order of Van Maanen 2, before any data reduction. The large scatter of points is not indicative of high instrument noise, but of noise introduced by the data reduction method and represents an error of about 5% in the center of the spectral order and 8% in the outer 5 – 10Å. These errors are typical for this method of echelle data reduction.

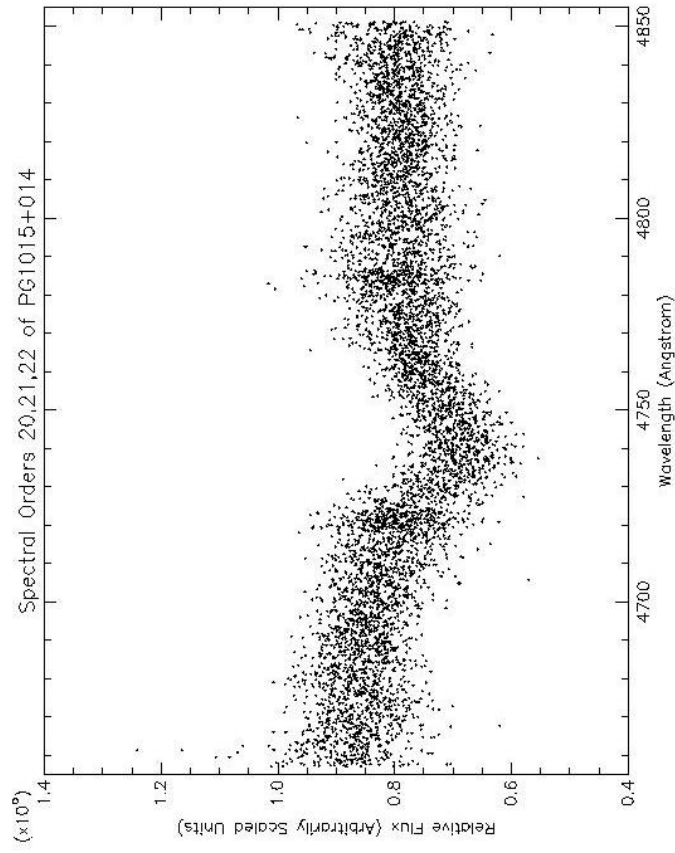


Figure 3.6: Spectral orders 20, 21, and 22 joined from PG1015+014 from the first night of observations. Note the shape of the absorption feature at 4740Å showing the characteristic spreading of the spectral line due to the presence of a strong magnetic fields.

Chapter 4

Discussion and Conclusions

The response transfer method of reducing echelle data has produced results, which while not as accurate across many spectral orders as those generated with the reference spectra method, seem promising. Several absorption features have been highlighted in the magnetic targets and the identification process has begun, albeit complicated by the varied effects of the magnetic field.

Van Maanen 2 has been demonstrated to be a good calibration tool for observations at wavelengths $\geq 4000\text{\AA}$. Although there are several ways to improve the quality of the output data. Taking reference spectra for vMA2 and the magnetic white dwarf targets could be used to benchmark the quality of the data by comparing this method to the reference spectra method.

In terms of future work on this project, it is likely that better results could be obtained by individually treating each spectral order and determining an appropriate degree of polynomial to fit. Also, using a different style of polynomial rather than just a basic may be appropriate to avoid the problem of diverging rapidly from the conversion ratio at the tails.

Intensive examination of the produced spectra could result in identification of more absorption features for analysis. Analysis of those features such as by studying the width and profile of absorption lines to characterize the magnetic field structure could lead to better constraints on the models for magnetic stellar atmospheres. [4] [3]

Bibliography

- [1] Angel, J. R. P., Liebert, J., and Stockman, H. S., 1985, *ApJ*, 292
- [2] Farihi, J. et al., 2004, *ApJ*, 608
- [3] Heyl, J.S., Reid, N., 1998, Keck Observing Proposal: HIRES Spectroscopy of Magnetic White Dwarf Stars
- [4] Heyl, J.S., Hernquist, L., 1998, *Phys. Rev. A*, 58, 3567
- [5] Hill, G. (site accessed Apr. 19-23th, 2007), High Resolution Echelle Spectrometer, W.M. Keck Observatory. (<http://www2.keck.hawaii.edu/inst/hires/hires.html>).
- [6] Putney, A., 1996, *ApJS*, 112
- [7] Schmidt, G.D. & Smith, P.S., 1995, *ApJ*, 448
- [8] Suzuki, N., et al., 2003, *PASP*, 115, 1050
- [9] Vogt, S. S. et al., 1987, *PASP*, 99, 1214
- [10] Vogt, S. S. et al., 1994, *Proc. SPIE*, 2198, 362
- [11] Weidemann, V. & Koester, D., 1989, *A&A*, 210